ISSN 1063-7834, Physics of the Solid State, 2021. © Pleiades Publishing, Ltd., 2021.
Russian Text © The Author(s), 2021, published in Fizika Tverdogo Tela, 2021, Vol. 63, No. 9, pp. 1228–1232.

SUPERCONDUCTIVITY

Electron Beam Lithography Fabrication of Superconducting Tunnel Structures

M. Yu. Fominskii[a], *, L. V. Filippenko[a], A. M. Chekushkin[a], and V. P. Koshelets[a]

[a] *Kotel'nikov Institute of Radio Engineering and Electronics, Russian Academy of Sciences, Moscow, 125009 Russia*

**e-mail: nanolith@yandex.ru*

Received April 9, 2021; revised April 9, 2021; accepted April 19, 2021

Abstract—An electron beam lithography technique for fabricating submicron Nb–AlN–NbN junctions has been developed and optimized. An exposure dose, development time, and plasma-chemical etching parameters that would ensure the maximum quality parameter of the R_j/R_n tunnel junctions have been selected. The use of negative resist ma-N 2400 with a lower sensitivity and better contrast as compared with resist UVN 2300-0.5 has made it possible to improve the reproducibility of the structure fabrication process and fabricate the submicron Nb–AlN–NbN tunnel junctions (an area from 2.0 to 0.2 μm^2) with a high current density and a quality parameter of $R_j/R_n > 15$. The spread of the parameters of the submicron tunneling structures over a substrate and the cycle-to-cycle reproducibility of the structure fabrication process have been experimentally measured.

Keywords: electron beam lithography, negative electron resist, plasma-chemical etching, magnetron sputtering, superconducting tunnel structure

DOI: 10.1134/S1063783421090067

1. INTRODUCTION

One of the most successfully developed areas of superconducting electronics is supersensitive terahertz receivers. An important task is the development of terahertz techniques and the creation of superconductor–insulator–superconductor (SIS) receivers with the quantum sensitivity and terahertz radiation sources for use in space and ground-based radio telescopes. Mixers based on the SIS tunnel junctions are the best input devices at frequencies from 0.1 to 1.2 THz; their noise temperature is only restricted by the quantum limit. Currently, the heterodyne SIS receivers are used as standard devices on most ground-based and space radio telescopes around the world [1, 2]. To implement the ultimate parameters of the SIS mixers, it is necessary to develop and optimize a reproducible and reliable technique for fabricating nanostructures with a tunnel barrier thickness of about 1 nm with an extremely high current density and low leakage currents [3–5]. To match to waveguide elements of a mixer, the area of junction with a high current density should be a fraction of a square micrometer. Electron lithography is one of the most promising methods for research nanostructure production, since it allows one to rapidly change the design of individual components and a chip as a whole and obtain the high reproducibility of results in the submicron tunnel junction size range.

To create a reproducible and reliable technique for fabrication of high-quality tunnel structures with good reproducibility and a small spread of parameters over a substrate, a technology based on direct electron beam lithography (EBL) and subsequent plasma-chemical etching for fabrication of the submicron Nb–AlN–NbN tunnel structures has been developed and adjusted.

2. EXPERIMENTAL

To study a technique for fabrication of submicron junctions, we prepared test samples with an array of circular cross-section structures separated by a distance exceeding the proximity effect range (Fig. 1) in different electron beam exposure, development, and etching modes. A SIS junction was formed on a silicon substrate by etching a Nb–AlN–NbN trilayer through a resistive film mask formed by electron lithography. The Nb–AlN–NbN trilayer was deposited on a Leybold L560UV facility equipped with a water-cooled substrate holder and two (DC and RF) magnetron sputtering systems. The niobium base electrode and a thin aluminum layer were deposited by DC magnetron sputtering in the argon atmosphere. After deposition of the aluminum barrier, the substrate was placed over an RF magnetron with an attached aluminum target and a plasma discharge was initiated in the nitrogen atmosphere [6]. After the completion of nitridation,

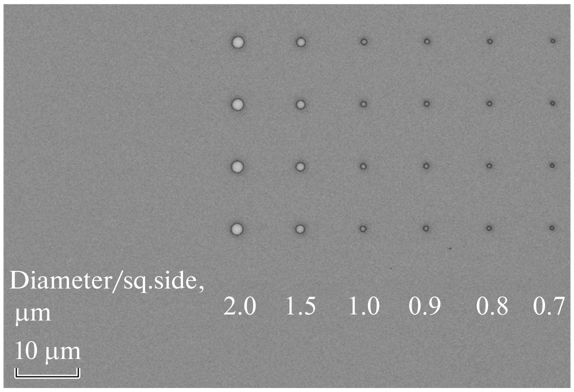

Fig. 1. Reference structure array for working out the modes of fabrication of submicron junctions.

the NbN counter electrode layer was deposited onto the barrier, which was formed by DC magnetron sputtering in argon and nitrogen. A scheme of the trilayer formation is given in Table 1.

After the formation of the junction by plasma-chemical etching, anodizing was performed; then, a SiO_2 insulating layer was deposited. The final stages are the formation of the NbN counter electrode and Au contact pads. Each stage of the tunnel junction formation was controlled by electron microscopy.

Negative resists of different types were used to form the junction geometry. Negative electron resist UVN 2300-0.5 has a high sensitivity and is used in both photolithography (DUV, 248 nm) and electron lithography. Negative electron resist UVN 2300-0.5 was deposited on the preliminarily formed Nb–AlN–NbN trilayer. After deposition, the resist was heat-treated at 90°C for 10 min. The resist film thickness was 0.38 μm. The exposure was carried out on a Raith e_LiNE electron lithography system by an electron beam with an electron energy of 30 keV; the dose ranged, depending on the junction size, from 8 to 20 $\mu C/cm^2$. After exposure, the samples were heated to 110°C for 10 min. Then, unexposed areas of the resist were removed in a 2.4% solution of tetramethylammonium hydroxide pentahydrate. Negative electron resist UVN 2300-0.5 has a low contrast; therefore, the technological process is highly sensitive to deviations, which affects the reproducibility of results. For resist UVN 2300-0.5, the following doses corresponding to the junctions with different specified sizes were selected (corrections took into account the deviations over the entire flow chart):

—a dose of 10 $\mu C/cm^2$ is optimal for the structures 2.0–1.5 μm in size;

—a dose of 15 $\mu C/cm^2$, for the structures 0.7–1.0 μm in size;

—and a dose of 20 $\mu C/cm^2$, for the structures 0.4–0.6 μm in size.

Thus, the junctions with an area of up to 0.15 μm^2 were fabricated and measured, but to increase the reproducibility of results and expand a technological window, other electron resists, in particular, ma-N 2400, were tested.

Negative resist ma-N 2400 is used in both photolithography (DUV, 248 nm) and electron lithography, but its sensitivity is lower than that of UVN 2300-0.5 by an order of magnitude; therefore, the resolution of ma-N 2400 for small areas will be higher. Negative electron resist ma-N 2400 was deposited onto the preformed Nb–AIN–NbN trilayer. After deposition, the resist was heat-treated at 90°C for 3 min. The electron beam lithography dose ranged from 110 to 275 $\mu C/cm^2$. The unexposed areas of the resist were removed in a 2.4% solution of tetramethylammonium hydroxide pentahydrate. To increase the etching resistance of the resistive mask, the samples after development were heated to 100°C for 10 min.

The use of negative resist ma-N 2400 (solid line in Fig. 2) with a lower sensitivity and better contrast as compared with UVN 2300-0.5 made it possible to improve the reproducibility of the structure fabrication.

Negative resist ma-N 2400 has a sensitivity lower than that of UVN 2300-0.5 by an order of magnitude and a better contrast. As can be seen from the measurement data (solid curves in Fig. 2), at exposure doses of 220 and 275 $\mu C/cm^2$, the size drifts are constant (in contrast to resist UVN 2300-0.5) and almost absent over the entire measurement range from 1.0 to 0.1 μm. For small (about 0.1 μm) diameters, the resolution of ma-N 2400 is higher.

Figures 3, 4, and 5 show electron microscope images of successive stages of fabrication of the structure with a diameter of 0.4 μm using resist ma-N 2400.

The junctions were formed by plasma-chemical etching of NbN using a resist mask (Fig. 3). The pro-

Table 1. Formation of a trilayer in a single vacuum cycle

Material	Description	Thickness, nm	Deposition parameters
Nb	Base electrode	200	DC, 600 W, Ar, 4 mTorr, 1.8 nm/s
Al	Tunnel barrier	6	DC, 100 W, Ar, 3 mTorr, 0.13 nm/s
AlN	Tunnel barrier	1.0–1.2	RF, 70 W, N_2, 0.03 mTorr
NbN	Counter electrode	80	DC, 600 W, Ar + N_2, 4 mTorr, 1.4 nm/s

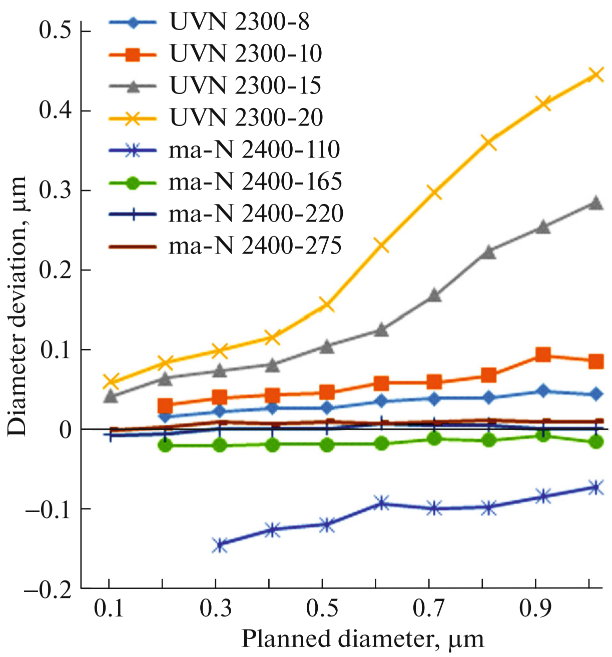

Fig. 2. Junction size drift during exposure and development (TMAH 2.4%, time 60 s) for resists ma-N 2400 and UVN 2300-0.5. The design diameter is along the horizontal axis. The difference in diameter of the structures measured on an electron microscope minus the design value is along the vertical axis. Positive values correspond to a diameter larger than that set in the fabrication.

cess occurs in a vacuum chamber of a Secon XPE II plasmachemical etching system in the O_2 and CF_4 gas mixture.

To obtain the high reproducibility and small spread of parameters, we studied the etching process and established optimal conditions for anisotropic etching of the NbN film with a minimum reproducible underetch (Fig. 4). The results of plasma-chemical etching were controlled on an electron microscope.

After the junction formation by plasma-chemical etching, anodization was performed, during which the niobium nitride film not covered by the resist transformed into the anodic oxide [7]. Next, a SiO_2 insulation layer was deposited (Fig. 5).

Figure 6 shows, for comparison, electron microscopy images of a structure with the same (0.4 μm) diameter, but based on resist UVN 2300-0.5. One can see the resist profile significantly different from the vertical profile (insufficient contrast of UVN 2300-0.5); the diameters of the resistive mask and the trilayer significantly differ from the design size.

The final technological stages are the formation of the NbN counter electrode and gold contact pads by photolithography using photoresist AZ 5214.

3. RESULTS

Several series of the submicron Nb–AlN–NbN junctions with a current density from 20 to 50 kA/cm^2 were fabricated. The measurements were performed on an IRTECON automated system for measuring the *I*–*V* characteristics and electrical parameters of SIS transitions. The *I*–*V* characteristics of the Nb–AlN–NbN junctions of the same size located in different parts of the substrate exhibited similar parameters. Figure 7 shows the *I*–*V* characteristics of the Nb–AlN–NbN junctions of the same size located in different parts of the same substrate. The measurements were performed on the junctions with areas of up to 0.15 μm^2, their quality did not change with decreasing sizes (Fig. 8).

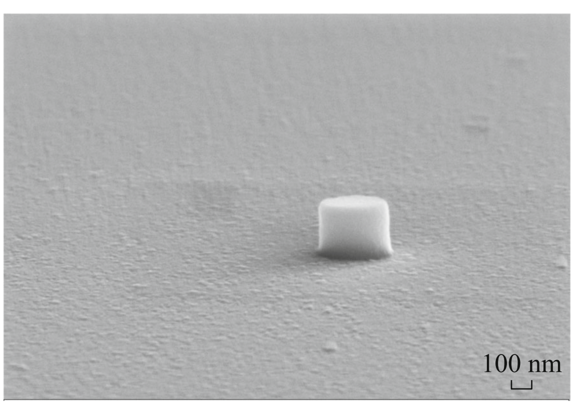

Fig. 3. Test junction based on resist ma-N 2400 with a diameter of 0.4 μm exposed at a dose of 220 μC/cm^2; after development, the diameter of the resist for forming the test junction is 0.37 μm.

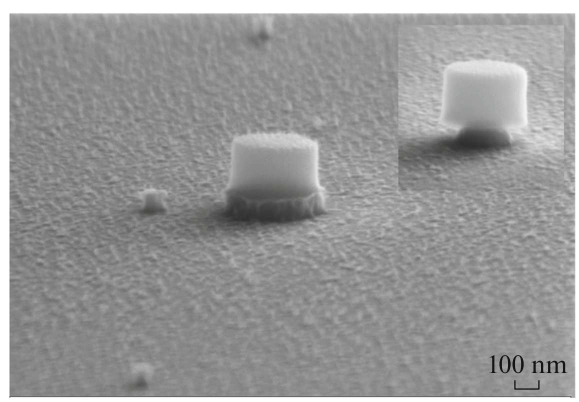

Fig. 4. Test junction based on resist ma-N 2400 with a diameter of 0.4 μm exposed at a dose of 275 μC/cm^2 after plasma-chemical etching over a resist mask in the CF_4 atmosphere. Inset: sample after etching in the CF_4 + O_2 atmosphere with nonoptimal parameters (the upper right corner). The resist diameter after etching was 0.33 μm in both cases.

Fig. 5. Test junction based on resist ma-N 2400 with a diameter of 0.4 μm after deposition of the SiO_2 insulation and "explosive" lithography.

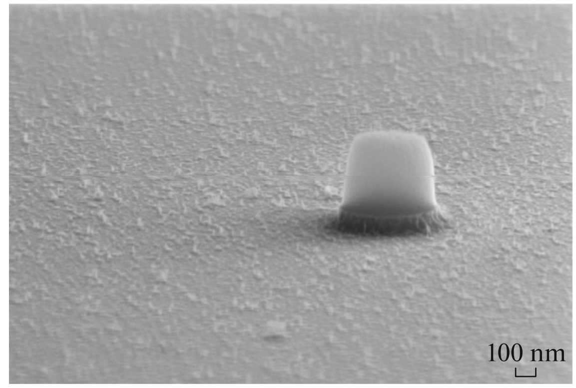

Fig. 6. Test junction based on resist UVN 2300-0.5 with a diameter of 0.4 μm exposed at a dose of 20 $\mu C/cm^2$ after plasma-chemical etching in the CF_4 atmosphere using a resist mask. The resistive mask diameter after etching is 0.46 μm and the trilayer diameter is 0.51 μm.

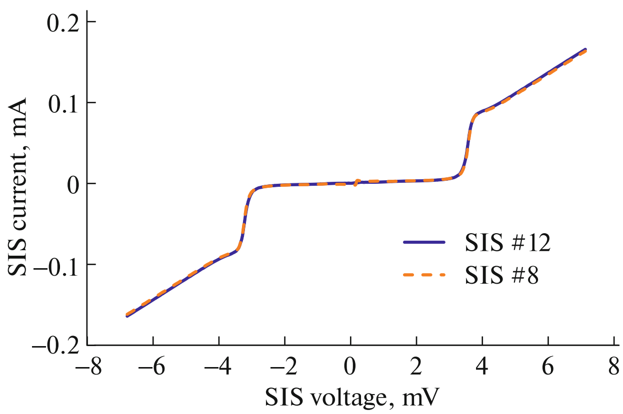

Fig. 7. *I–V* characteristics of the Nb–AlN–NbN junctions of the same size fabricated by electron beam lithography located on different parts of the same substrate: SIS no. 8 with an area of 0.480 μm^2, a current density of 15 kA/cm^2, R_n = 40.98 Ω, R_j/R_n = 18.4, and V_g = 3.39 mV; SIS no. 12 with an area of 0.488 μm^2, a current density of 15 kA/cm^2, R_n = 40.34 Ω, R_j/R_n = 20.7, and V_g = 3.38 mV.

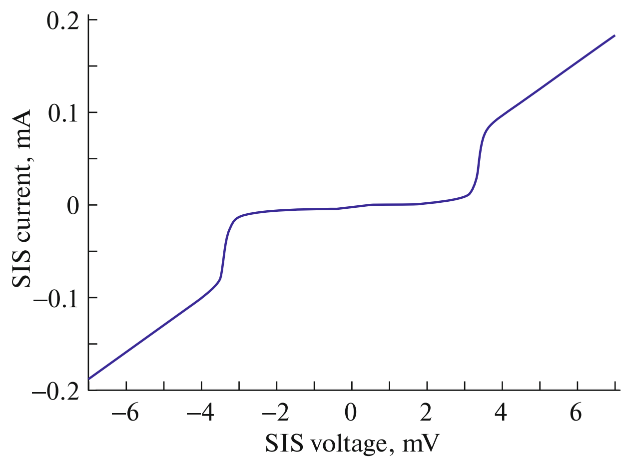

Fig. 8. *I–V* characteristic of the Nb–AlN–NbN junction with an area of 0.15 μm^2, a current density of 47 kA/cm^2, R_n = 34.53 Ω, R_j/R_n = 21.1, and V_g = 3.36 mV fabricated by electron beam lithography and plasma-chemical etching.

4. CONCLUSIONS

A technique for fabricating the submicron Nb–AlN–NbN junction using electron beam lithography was developed and adjusted. A high-quality ultrathin AlN barrier was formed by nitridation of the Al surface in an RF plasma discharge in the pure N_2 atmosphere. An exposure dose, development time, and plasma-chemical etching parameters ensuring the maximum quality parameter of the R_j/R_n tunnel junctions were selected. Along with investigations of negative resist UVN 2300-0.5, the parameters of negative resist ma-N 2400 were selected, which has a sensitivity lower than that of UVN 2300-0.5 by an order of magnitude and a better contrast. Each stage of the tunnel junction formation was controlled by electron microscopy. This made it possible to fabricate the submicron Nb–AlN–NbN tunnel junctions (an area from 2.0 to 0.2 μm^2) with the high current density and a quality parameter of $R_j/R_n > 15$. The spread of the parameters of the submicron tunnel structures over the substrate and the cycle-to-cycle reproducibility of the structure fabrication process were experimentally measured.

FUNDING

This study was supported by the Russian Science Foundation, project no. 19-19-00618. The tunnel structures were fabricated at the Kotel'nikov Institute of Radio Engineering and Electronics within the state assignment using a UNU 352529 large-scale research facility.

CONFLICT OF INTEREST

The authors declare that they have no conflicts of interest.

REFERENCES

1. B. D. Jackson, G. de Lange, T. Zijlstra, M. Kroug, J. W. Kooi, J. A. Stern, and T. M. Klapwijk, IEEE Trans. Microwave Theory Technol. **54**, 547 (2006).
2. A. Karpov, D. Miller, F. Rice, J. A. Stern, B. Bumble, H. G. LeDuc, and J. Zmuidzinas, IEEE Trans. Appl. Supercond. **17**, 343 (2007).
3. K. I. Rudakov, P. N. Dmitriev, A. M. Baryshev, A. V. Khudchenko, and V. P. Koshelets, Russ. Phys. J. **59**, 711 (2016).
4. M. Yu. Torgashin, V. P. Koshelets, P. N. Dmitriev, A. B. Ermakov, L. V. Filippenko, and P. A. Yagoubov, IEEE Trans. Appl. Supercond. **17**, 379 (2007).
5. P. N. Dmitriev, I. L. Lapitskaya, L. V. Filippenko, A. B. Ermakov, S. V. Shitov, G. V. Prokopenko, S. A. Kovtonyuk, and V. P. Koshelets, IEEE Trans. Appl. Supercond. **13**, 107 (2003).
6. B. Bumble, H. G. LeDuc, J. A. Stern, and K. G. Megerian, IEEE Trans. Appl. Supercond. **11**, 76 (2001).
7. X. Meng and T. van Duzer, IEEE Trans. Appl. Supercond. **13**, 91 (2003).

Translated by E. Bondareva